Bulletin Géodésique (1993) 67:210–223

Bulletin Géodésique

A proposed GPS method with multi-antennae and single receiver

Rock Santerre [1] **and Gerhard Beutler** [2]

[1] Centre de recherche en géomatique, Université Laval, Québec, Canada G1K 7P4
[2] Astronomisches Institut, Universität Bern, CH-3012 Bern, Switzerland

Received February 3, 1993; Accepted April 21, 1993

Abstract. A method based on multi-antennae linked to a common GPS receiver is proposed. The goal of the technique is to improve height determination for baselines a few kilometres in length. The advantage of this technique resides in the elimination of relative clock parameters in the "between-antenna" single difference observations. Because single difference observations are free of clock errors more geometrical strength remains to determine the baseline components. This statement is valid as long as intercable biases can be carefully calibrated. For millimetre height determination, the intercable calibration must be done at the same level of accuracy. Under this assumption it is shown that in general the height standard deviation improves by a factor of about three compared to standard GPS data processing. With the proposed method, the effect of relative tropospheric zenith delay errors becomes a bit smaller (in absolute value), compared to standard data processing. To absorb this error, a relative tropospheric zenith delay parameter may be estimated. Even with this additional parameter in the solution the height standard deviation remains two times smaller than the results of standard processing techniques (without tropospheric zenith delay parameter), and at least five times smaller than in the results obtained from standard processing including one tropospheric zenith delay parameter.

1. INTRODUCTION

It is well known that GPS (ellipsoidal) height determination is weaker than that of horizontal coordinates. The confidence ellipsoid, inferred from the covariance matrix of a GPS least squares adjustment, is elongated along (or close to) the zenith direction (Santerre 1991). This means that random measurement errors propagate more adversely into the vertical coordinate than into the horizontal ones. This is why repeatability studies show less consistent results for height determinations than for the horizontal components. For example, Gurtner et al. (1989) have reported, for two annual GPS campaigns, agreement of about 2 mm in horizontal GPS position with the terrestrial solution. For the height determination, the best agreement was about 5 mm, due to perturbing effects of the troposphere. The formal accuracy of the horizontal coordinates was twice as high as that of the height component.

The weakness of GPS height determinations can explained by the following facts: i) a high degree of correlation exists between the vertical coordinate and the clock parameters, as well as with the tropospheric delay parameters; ii) GPS satellites are only visible above the local horizon.

With the standard GPS field operation, clock parameters may be explicitly estimated in a GPS least squares adjustment with between-receiver single difference observations or they may be implicitly taken into account with a double difference observations processing scheme. The standard field operation consists of two or more receivers operating simultaneously without physical links between them. The proposed field operation consists of two or more antennae connected to the same receiver. In this scenario, the between-antenna single difference observation does not contain receiver clock errors.

Correspondence to: R. Santerre

This statement holds only if a careful calibration of the relative signal delay throughout the hardware (antennae, cables, receivers) is performed. If this latter condition is met, no clock parameter has to be estimated.

The goal of the proposed method is to improve height determination for small monitoring network (e.g., dam deformation monitoring). The small area covered by those networks facilitates the deployment of (fiber optic) cables to link several antennae to one common receiver. The cables could be permanently set-up and be part of a continuous deformation monitoring system. Continuous deformation monitoring systems are already in operation. For example, DeLoach (1989) uses fiber optic cables (permanently installed inside a dam) for data transmission between the receivers and the computer. This fiber optic cable network could be used to connect multiple antennae to one receiver located next to a computer. The proposed method would solve the data link problem and improve GPS height determination at the same time.

There are already receivers available controlling more than one antennae (Jurgens and Rodgers 1991; Qin et al. 1992). The main purpose of these receivers is attitude control of a platform. To ensure the success of the proposed field operation with these commercial receivers, careful calibration of relative delay throughout hardware would have to be done.

Single difference processing (without clock parameters estimation) of observations has already been proposed by MacDoran (Schreiner 1990). In their scenario, the observations are collected by receivers linked to a common oscillator. The receivers and the oscillator are located at a common site. Every antenna located on a geodetic point is connected to its receiver with a fiber optic cable. The purpose of their set-up is satellite orbit determination using a network with baseline lengths of about 100 km.

This paper is a theoretical study to prove the advantage of the proposed method over the standard field operation and data processing. To demonstrate the usefulness of the proposed field operation to improve height determination, the following topics will be addressed. First, the observation equations are reviewed in section 2. This section also discusses error modelling with emphasis on intercable bias calibration. In the third section, simulation results are presented and analysed. For the proposed method, the impact of the propagation of intercable bias into station coordinates is studied. Finally, the propagation of systematic tropospheric errors and random measurement errors into GPS station coordinates for the proposed method is compared to standard data processing.

2. OBSERVATION EQUATIONS AND ERROR MODELLING

2.1 Observation equations

The observation equation relates the observables and the estimated parameters (both desired and nuisance parameters). Let us start with the observation equation of the basic undifferenced carrier beat phase. This is the fundamental GPS carrier phase observation equation from which any other linear combination of observations can be created. For the purpose of the proposed method, all the errors related to receiver (antenna and cable) are explicitly included in the observation equations.

The undifferenced carrier phase observation equation can be written as follows:

$$\Phi = \rho - c\cdot dt - \lambda\cdot\phi^0 - d^{ec} - dio + dtr + dmp + dpc + dan + dca + dec + dch + c\cdot dT + \lambda\cdot\phi_0 + \lambda\cdot N + v \qquad (1)$$

$$\rho = \| \mathbf{r} - \mathbf{R} \|$$

where,

- Φ : carrier phase observable (in length units)
- ρ : geometric range between satellite and receiver (or antenna)
- c : vacuum speed of light
- dt : satellite clock error
- λ : carrier wavelength
- ϕ^0 : initial phase of satellite oscillator
- d^{ec} : range error due to delay in satellite electrical circuit
- dio : range error due to ionospheric refraction
- dtr : range error due to tropospheric refraction
- dmp : range error due to multipath effect
- dpc : range error due to antenna phase centre variation
- dan : range error due to delay in antenna (including amplifier)
- dca : range error due to delay in antenna cable
- dec : range error due to delay in receiver (the common electrical circuit for all signals)
- dch : range error due to delay in receiver channel
- dT : receiver clock error
- ϕ_0 : initial phase of receiver oscillator
- N : integer carrier phase ambiguity
- v : carrier phase observation noise

In the observation equation (1) as well as in the other observation equations below, it is assumed that the receiver clock is synchronized to GPS time within 1 μsec or that this synchronization is known to within 1 μsec. This can be instantaneously achieved from absolute point positioning solutions using pseudorange measurements collected at one epoch from at least 4 satellites. The geometric range ρ contains implicitly the receiver (antenna) position vector **R** at the receiving time and the satellite position vector **r** at the transmitting time. The range error due to satellite orbit bias ($d\rho^S$) enters in the calculation of the misclosure vector (see eqn. 7 below).

The (between-receiver or between-antenna) single difference carrier phase observation equation (Figure 1a) is:

$$\Delta\Phi = \Delta\rho - \Delta dio + \Delta dtr + \Delta dmp + \Delta dpc + \Delta dan + \Delta dca + \Delta dec + \Delta dch + c\cdot\Delta dT + \lambda\cdot\Delta\phi_0 + \lambda\cdot\Delta N + \Delta v \quad (2)$$

where, Δ is the between-receiver (between-antenna) single difference operator. In relative positioning the coordinates of one station have to be fixed, the range error due to offsets in the coordinates of the fixed station ($d\rho_R$) also enters in the calculation of the misclosure vector (see eqn. 7 below).

The advantages of the (between-receiver or between-antenna) single differences are the removal of the satellite clock error (dt), the initial phase of satellite oscillator (ϕ^0), and the delay in satellite electrical circuit (d^{ec}). Because of the positive spatial correlation, the effects of orbit errors and propagation (ionospheric and tropospheric) errors are greatly reduced. On the other hand, those errors that are uncorrelated between receivers are increased (e.g., multipath and measurement noise).

Estimating one clock parameter at each observation epoch (or processing the observations in double difference mode) eliminates errors common to all observations at that epoch. These errors are the relative receiver clock (ΔdT), the relative initial phase of receiver oscillator ($\lambda\cdot\Delta\phi_0$), the relative antenna delay (Δdan), the relative cable delay (Δdca), and the relative receiver circuit (excluding channel) delay (Δdec).

The (receiver-satellite or antenna-satellite) double difference carrier phase observation equation is:

$$\nabla\Delta\Phi = \nabla\Delta\rho - \nabla\Delta dio + \nabla\Delta dtr + \nabla\Delta dmp + \nabla\Delta dpc + \nabla\Delta dch + \lambda\cdot\nabla\Delta N + \nabla\Delta v \quad (3)$$

where ∇Δ is the double difference operator.

Double differencing is one of the most widely used techniques of operational software (Rothacher et al. 1990; Santerre 1988).

If two (or more) antennae are connected to a single receiver, see Figure 1b, the terms (dT), (dec) and (ϕ_0), in eqn. (1), are the same for the observations collected by the two antennae. Then, the following modified single-difference observation equation can be written:

$$\Delta\Phi = \Delta\rho - \Delta dio + \Delta dtr + \Delta dmp + \Delta dpc + \Delta dan + \Delta dca + \Delta dch + \lambda\cdot\Delta N + \Delta v \quad (4)$$

If the relative antenna delay (Δdan) and the relative cable delay (Δdca) can be carefully calibrated, it is therefore not necessary to solve for clock parameters. This means that the high correlation between the receiver clock and the baseline height component (and the tropospheric delay parameter) vanishes. This will eventually lead to a better GPS height determination.

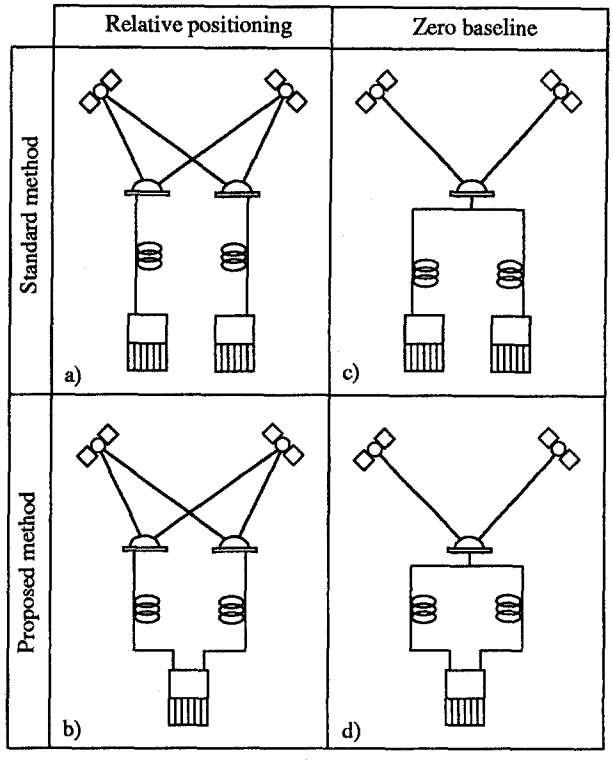

Figure 1. Illustration of the standard and the proposed methods.

2.2 Error modelling

Let us now comment about the error terms contained in the observation equations, and how some of those errors can be reduced to a negligible level for short baselines (a few kilometres in length).

Typically, an error of 1 ppm (dr/ρ) in satellite orbit produces a maximal error of 1 ppm (db/b) in baseline vector **b**. The error of broadcast orbit is of the order of 0.5 ppm (Remondi and Hofmann-Wellenhof 1989). However, with selective availability (SA) activated, broadcast orbit errors can reach 5 ppm (Tolman et al. 1990). Post-computed precise orbits better than 0.1 ppm (Beutler 1992) reduced, to a negligible level, the impact of satellite orbit error on short baselines.

Satellite clocks are also dithered if selective availability is turned on. According to Rocken and Meertens (1991), clock dithering (at ±2 Hz) has no significant effect on relative positioning as long as the receiver clocks are synchronized to better than 10 msec.

The major effect of ionospheric refraction is a baseline contraction by a factor of -0.6 ppm for a Total Electron Content (TEC) of 10^{17} el/m^2 (Santerre 1991). The effect is proportional to the actual TEC value. TEC values range between 10^{16} to $2x10^{18}$ el/m^2. With dual frequency receivers this effect may be removed by forming the so-called ionospheric-free linear combination. Instead of using this combination which leads to an observable with a three times higher noise than the L1 observables, it is preferable on short baselines to apply ionospheric correction to the L1 observation from a deterministic ionospheric model. Wild et al. (1989) and Georgiadou (1990) have developed such a model which used dual frequency carrier phase observables to map TEC values as functions of sun right ascension and latitude of ionospheric point. Georgiadou (1990) has shown that the remaining ionospheric effect on baselines was below 0.2 ppm.

Tropospheric refraction, especially the wet path delay induced from the water vapour content, is one of the most difficult errors to model. For example, each 1 mm of relative tropospheric zenith delay mismodelling creates an error of about 3 mm in the baseline height component (Santerre 1991). Large height differences between sites or local meteorological phenomena (e.g., temperature inversions) lead to errors significant even on short baselines. The estimation of a tropospheric delay parameter can take into account unmodelled tropospheric error. However, this additional parameter is highly correlated with the baseline height component and the receiver clock parameter (in standard data processing). The proposed method is designed to solve this dilemma (see below).

Multipath is caused by the reflection of GPS signal on objects located nearby the antenna. The effect on the carrier phase observation may reach a magnitude equal to one quarter of the carrier wavelength (i.e., 5 cm on L1) (Georgiadou and Kleusberg 1988). Careful selection of observing sites to avoid the vicinity of reflective objects, radiowave absorbing material deployed around the antenna, and choke-ring antenna are possible ways to reduce multipath effects on the observations. Moreover, to diminish multipath effects on baseline components, it is recommanded to collect data for time spans longer than the period of the cyclic multipath phenomena.

Relative phase centre variations of "identical" antenna is usually less than 5 mm (Geiger 1990). Tranquilla and Colpitts (1989) suggested the calibration of antenna phase centre variation in anechoic chambers. Such a calibration allows to take into account this effect at the mm-level. With the proposed method, relative signal delays throughout the antenna (and the low noise amplifier) has to be dealt with. Technically, this calibration could be done as precisely as the phase center variation calibration.

Interchannel errors do not exist for receivers with sequencing channel or multiplexing channel. Most of the commercial receivers have multiple channels however. The interchannel bias is usually no problem in modern receivers, as this calibration is accomplished by the receiver's microprocessor. Thomas (1988), e.g., reports that the Rogue receiver has an interchannel bias of 0.2 mm or less for carrier phase observations.

For short baselines (a few kilometres), carrier phase ambiguities can easily be fixed to their integer values even with rather short data spans (Frei and Beutler 1990). The

ability to fix carrier phase ambiguity parameters to integer values in the least squares adjustment process is primordial to achieve a high level of positioning accuracy. For this reason, the simulation results in section 3 assume ambiguities-fixed solutions.

Offsets in the coordinates of the fixed station introduce errors into the determination of the baseline components. Santerre (1991) has shown that each 10 m of offset in the height of the fixed station mainly produces a -0.3 ppm error in horizontal baseline components. For each 10 m of offset in the horizontal coordinates of the fixed station, the error in baseline height component (proportional to baseline length) can reach 0.4 ppm. To reduce this error it is suggested to connect tridimensionally the fixed station to existing geodetic networks.

With the proposed method, the remaining term to deal with is the relative cable delay. Zero-baseline tests are well suited to calibrate this delay. In these tests, the signals collected by one antenna are split to feed the cables connected to the same receiver. The single difference observables give the intercable calibration value, as long as the interchannel delay is negligeable (see above) or known.

The zero baseline single difference carrier phase observation equation for the proposed method (Figure 1d) is:

$$\Delta\Phi = \Delta dca + \Delta dch + \Delta v \qquad (5)$$

With the standard method, the zero baseline test is a way to assess measurement noise and residuals interchannel error (in double difference processing).

The zero baseline double difference carrier phase observation equation (Figure 1c) is:

$$\nabla\Delta\Phi = \nabla\Delta dch + \nabla\Delta v \qquad (6)$$

The major problem in calibrating the term (Δdca) in eqn. (5) is the change of cable length due to temperature variations. Table 1 presents typical values of thermal coefficient of delay for different type of cables. The technical details about fiber optic technology given in the next paragraphs stem from the following papers: (Young 1991; Logan et al. 1990; Primas et al. 1990).

Table 1. Cable thermal coefficient of delay (TCD) and change of cable length as a function of cable length (L).

Type	TCD (ppm/°C)	change of cable length (mm/°C) L : 10 m	100 m	1 km	2 km
coaxial RG-58	-175	-1.8	-17.5	-175	-350
coaxial RG-331	-30	-0.3	-3.0	-30	-60
single mode f.o.	7	0.07	0.7	7	14
LTC f.o.	0.5†	0.005	0.05	0.5	1.0
LTC f.o.	0.1*	0.001	0.01	0.1	0.2

LTC: low thermal coefficient,† at 35°C, * between 10° & 25°C
f.o.: fiber optic

Coaxial cables of 1 km in length experience length changes of many centimetres per 1°C of temperature variation. Fiber optic cables however have much lower thermal coefficients than coaxial cables. Specially design fiber optic cables have coefficient smaller than 0.5 ppm/°C, the diameter of such cables being about 2 cm.

For dam deformation application, the cables could run inside the galleries. The outdoor part of the cable could be thermally isolated. Knowledge of the thermal coefficient of delay allows to apply correction, if the temperature is measured at different points along the cable route.

For practical considerations, the separation between the antennae and the receiver must be, at least, of the order of a few kilometres. Typical cable loss values and the percentage of power remaining at the end of a cable for different cable length are presented in Table 2. Once again the performance of fiber optic is better than coaxial cable.

Table 2. Cable loss and remaining power as a function of cable length (L).

Type	loss (dB/km)	remaining power L : 10 m	100 m	1 km	2 km
coaxial	100	79%	10%	-	-
coaxial	50	89%	32%	-	-
coaxial	20	95%	50%	1%	-
fiber optic	0.5	99.9%	99%	89%	79%
fiber optic	0.25	99.9%	99.4%	94%	89%

The symbol "-" indicates that the remaining power is less than 1%.

In addition to its low thermal coefficient and its low attenuation, fiber optic cables are not affected by

electromagnetic interference (and do not produce interference) and have excellent stability properties (10^{-15}). However, the choice of fiber optic cables means modifications to actual receiver hardware. The components to be added are: i) one light source at the receiver site; ii) one light modulator to modulate the optical carrier with the electrical GPS signal at each antenna; and iii) one demodulator at the receiver input. Because different modulators are used at the different antennae, the relative delay introduced by the modulators must be calibrated. With a light source at the receiver, in-situ relative cable delays could be measured, if precise time differences (psec) between the two-way light travel time within each cable are measured.

To assess the necessary level of accuracy for the calibration of the relative cable delay in order to achieve mm-accuracy in the baseline components, simulations are presented in the next section. Moreover, to demonstrate the usefulness of the proposed method, the error propagation into the station coordinates will be analysed and compared with respect to the results obtained from the standard method. The analyzed errors are the systematic tropospheric delay and the measurement noise, i.e., the remaining errors affecting short baselines (as explained above).

3. ERROR PROPAGATION INTO STATION COORDINATES

3.1 Simulation technique

The simulation technique used in this paper is that outlined by Geiger (1988), further developed, applied and documented by Santerre (1989; 1991). The starting point is the normal equation system for single difference processing:

$$\mathbf{x} = (\mathbf{A}^T\mathbf{A})^{-1}\,\mathbf{A}^T\mathbf{W} = \mathbf{N}^{-1}\,\mathbf{U} \qquad (7)$$

where,
x : vector containing the unknown parameters
A : partial derivative matrix of the problem
W : vector containing the considered biases of the observations ($\varepsilon\Delta\Phi$)

In the usual least squares procedures **W** is the vector containing the terms "observed minus computed", the so called misclosure vector. Single difference observations are assumed to be independent and of equal weight.

For standard single difference processing schemes (eqn. 2) the vector x is modelled as:

$$\mathbf{x} = (dx, dy, dz, c{\cdot}\Delta dT) \qquad (8a)$$

where: dx, dy, dz are the estimated increments to the initial value of the baseline vector. To facilitate the interpretation of the simulation results, the components refer to the local geodetic "north-east-up" system. The term $c{\cdot}\Delta dT$ is the synchronization error between the two receiver clocks expressed in metres.

For the proposed method clock parameters do not have to be introduced. This means that in the single difference processing (eqn. 4) the vector x is modelled as:

$$\mathbf{x} = (dx, dy, dz) \qquad (8b)$$

Optionally, a relative tropospheric zenith delay parameter ($\Delta dtr(0)$) can be taken into account in the simulation scheme. In this case, equations (8a) and (8b) are augmented, respectively, as follows:

$$\mathbf{x} = (dx, dy, dz, c{\cdot}\Delta dT, \Delta dtr(0)) \qquad (8c)$$
$$\mathbf{x} = (dx, dy, dz, \Delta dtr(0)) \qquad (8d)$$

The individual terms in the normal equation system are now computed analytically assuming that the satellite sky distribution is homogeneous. A homogeneous satellite sky distribution means that the number of observations by area units (surface density) is constant over the observer's sky. A similar simulation technique, assuming homogeneous distribution of satellites within a solid angle above the observer has also been used by Sjöberg (1992).

$$\mathbf{N} = \begin{pmatrix} N_{11} & N_{12} & N_{13} & N_{14} & N_{15} \\ N_{21} & N_{22} & N_{23} & N_{24} & N_{25} \\ N_{31} & N_{32} & N_{33} & N_{34} & N_{35} \\ N_{41} & N_{42} & N_{43} & N_{44} & N_{45} \\ N_{51} & N_{52} & N_{53} & N_{54} & N_{55} \end{pmatrix} ; \quad \mathbf{U} = \begin{pmatrix} U_1 \\ U_2 \\ U_3 \\ U_4 \\ U_5 \end{pmatrix} \qquad (9a)$$

where,

$$N_{ik} = [e_i\ e_k] \quad \text{and} \quad U_i = [e_i\ \varepsilon\Delta\Phi] \qquad (9b)$$

[...] means the summation over all observations (from all satellites and epochs for the whole session), and e_i are the elements of the design matrix A, namely:

$$
\begin{aligned}
e_1 &= -\sin\zeta\cos\alpha \\
e_2 &= -\sin\zeta\sin\alpha \\
e_3 &= -\cos\zeta \\
e_4 &= 1 \\
&\text{and optionally,} \\
e_5 &\approx \cos^{-1}\zeta
\end{aligned}
\qquad (9c)
$$

Depending on the selected parameters to be solved for, only the associated elements of matrix **N** and vector **U** are accumulated for the entire observing session. For each systematic error to be studied, analytical expressions $\varepsilon\Delta\Phi(\alpha,\zeta)$ which represent the bias introduced in the single difference observation by the selected systematic error have been developed. For the mathematical development of these expressions the reader is referred to Santerre (1989 App. II).

The summations in equations (9b) are now replaced by double integrals (over azimuths and zenith angles), assuming a homogeneous satellite distribution within the area defined by the integration boundaries.

In practice, during the processing of real GPS data in single difference mode one clock parameter is estimated per epoch. According to eqn. (8a) only one such parameter is introduced here for the entire adjustment. This is theoretically equivalent to assuming that all observations were made simultaneously. It can be mathematically proven that, if the number of observations at epoch "j" (n_j) and the $[e_4 e_i]^{nj}$ terms (the summation over the number of observations at epoch "j") are equal to those of epoch "j+1": (n_{j+1}) and $[e_4 e_i]^{nj+1}$, respectively, the estimation of one clock parameter by session or one clock parameter by epoch will not alter the part of the covariance matrix related to station coordinates. Furthermore if $[e_4 \varepsilon\Delta\Phi]^{nj}$ equals $[e_4 \varepsilon\Delta\Phi]^{nj+1}$, the propagation of systematic error into station coordinates will not be affected.

These assumptions are not always satisfied but they represent a fair approximation to the reality (Santerre 1991). With the future 24 satellite constellation these assumptions will be even more realistic.

The method proved to be very powerful to describe the propagation of random observation errors and systematic errors into the estimated station coordinates (Santerre 1991). Simulation results agree with real data processing results to better than 75%. This is considered acceptable to get a good feeling about general trends of error propagation into station coordinates. The advantages of this simulation technique over the conventional simulation technique are: i) fast generation of simulation results; and ii) general trends of error propagation are easily achieved.

3.2 Simulation scheme

A general study of the propagation of systematic errors (constant delay and tropospheric delay) and the behaviour of the confidence ellipsoids has been carried out as a function of the selected parameters in the least squares adjustment. The impact of satellite sky distribution and elevation mask angle has also been studied. The three selected satellite sky distributions are representative for the expected satellite configurations for the equatorial (ϕ=0°), mid-latitude (ϕ=45°) and polar (ϕ=90°) sites when the complete GPS constellation will be in place. Illustrations of these satellite configurations are presented in Figure 2. The equatorial site is very well covered by satellite observations. However, for mid-latitude sites a lack of observations is present between azimuths 315° and 45°. For polar sites, only observations at low elevation angles (below 45°) are possible.

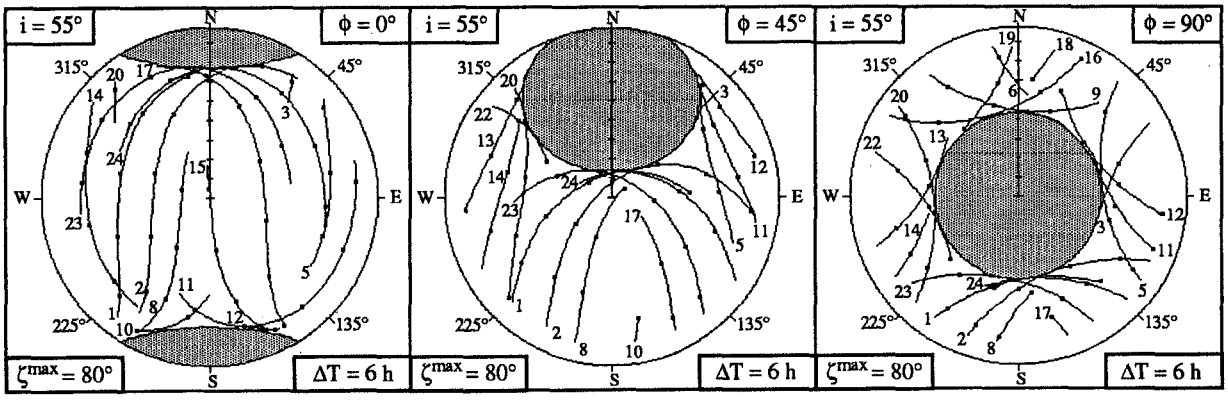

Figure 2. Typical satellite sky distributions as a function of site latitude.

Previous observation campaigns, where the constellation contained less satellites, might have produced less favourable satellite sky distributions.

The simulations assume ambiguities-fixed solutions. Results for the ambiguities-free solutions, where the carrier phase ambiguities are estimated in the least squares adjustments, may be quite different, see (Santerre et al. 1990; Santerre and Lavoie 1991), but they are of no importance for the purpose of this paper.

3.3 The effect of a constant delay error (e.g., intercable bias)

First, simulations have been made to study the propagation of a constant delay error into station coordinates. For the proposed method, the main effect of intercable bias is manifested by a translation (of the free station) along the z-axis (Tz) proportional to the intercable bias. Results are presented in Tables 3a, 3b and 3c, for equatorial, mid-latitude and polar sites, respectively. The simulations have been performed for the proposed method without a tropospheric delay parameter (eqn. 8b) and with a tropospheric delay parameter (eqn. 8d). ζ^{max} represents the maximun zenith angle. For an elevation mask angle of 20°, ζ^{max} equals 70°.

Table 3a. Effects on station coordinates due to each 1 mm of intercable bias for equatorial site. Proposed method without (line 2) and with (line 3) a tropospheric delay parameter.

ζ^{max} :	65°	70°	75°	80°	85°	
Tz :	-1.33	-1.38	-1.42	-1.46	-1.49	(mm)
Tz :	-0.73	-0.78	-0.86	-0.95	-1.10	(mm)

Table 3b. Effects on station coordinates due to each 1 mm of intercable bias for mid-latitude site. Proposed method without (lines 2&3) and with (lines 4&5) a tropospheric delay parameter.

ζ^{max} :	65°	70°	75°	80°	85°	
Tz :	-1.30	-1.33	-1.36	-1.39	-1.40	(mm)
Tx :	0.15	0.18	0.22	0.26	0.31	(mm)
Tz :	-0.73	-0.78	-0.86	-0.95	-1.09	(mm)
Tx :	0.01	0.01	0.02	0.03	0.06	(mm)

Table 3c. Effects on station coordinates due to each 1 mm of intercable bias for polar site. Proposed method without (line 2) and with (line 3) a tropospheric delay parameter.

ζ^{max} :	65°	70°	75°	80°	85°	
Tz :	-1.73	-1.83	-1.93	-2.02	-2.09	(mm)
Tz :	-0.89	-0.97	-1.08	-1.22	-1.44	(mm)

For the proposed method without a tropospheric zenith delay parameter (eqn. 8b), the effects of intercable bias can be summarized as follows (the range is for elevation mask angles of 20° and 10°, respectively):

- For equatorial sites, the magnification factor ranges from -1.4 to -1.5;
- For mid-latitude sites, the magnification factor ranges from -1.3 to -1.4. In addition, horizontal translations along the x-axis (Tx, x: north component) ranges from 0.2 to 0.3;
- For polar sites, the magnification factor ranges from -1.8 to -2.0.

For the proposed method with a tropospheric zenith delay parameter (eqn. 8d), the effects of intercable bias can be summarized as follows:

- For equatorial sites, the magnification factor ranges from -0.8 to -1.0;
- For mid-latitude sites, the magnification factor ranges from -0.8 to -1.0. Horizontal translations along the x-axis (north component) also exist but they are insignificant;
- For polar sites, the magnification factor ranges from -1.0 to -1.2.

The above results show that in order to perform mm-level surveys, the intercable calibration must be achieved at the mm-level. The effect on station height is not greatly amplified, as one could imagine having in minds that the VDOP (Vertical Dilution Of Precision) factor may reach values up to 6, even with the complete satellite constellation. The DOP factors are uniquely based on one epoch of observations; there should not be used to evaluate the strength of satellite sky distribution for a complete session. Moreover, DOP factors do not give at all any indication about the way systematic errors propagate into the station coordinates.

3.4 The effect of a tropospheric zenith delay error

The main effect of a tropospheric zenith delay error is a translation (of the free station) along the z-axis (Tz) proportional to the tropospheric zenith delay error. Results are presented in Tables 4a, 4b and 4c, for equatorial, mid-latitude and polar sites, respectively, using the standard and the proposed methods.

Table 4a. Effects on station coordinates due to each 1 mm of tropospheric zenith delay error for equatorial site. Standard (line 2) vs proposed (line 3) methods.

ζ^{max} :	65°	70°	75°	80°	85°	
Tz :	2.18	2.59	3.19	4.18	6.16	(mm)
Tz :	-1.87	-2.05	-2.26	-2.48	-2.71	(mm)

Table 4b. Effects on station coordinates due to each 1 mm of tropospheric zenith delay error for mid-latitude site. Standard (lines 2&3) vs proposed (lines 4&5) methods.

ζ^{max} :	65°	70°	75°	80°	85°	
Tz :	2.19	2.59	3.19	4.19	6.18	(mm)
Tx :	-0.01	-0.01	-0.02	-0.04	-0.09	(mm)
Tz :	-1.76	-1.90	-2.03	-2.15	-2.18	(mm)
Tx :	0.46	0.61	0.82	1.16	1.78	(mm)

Table 4c. Effects on station coordinates due to each 1 mm of tropospheric zenith delay error for polar site. Standard (line 2) vs proposed (line 3) methods.

ζ^{max} :	65°	70°	75°	80°	85°	
Tz :	3.23	3.87	4.86	6.51	9.92	(mm)
Tz :	-3.06	-3.48	-3.98	-4.56	-5.19	(mm)

For the standard data processing scheme (eqn. 8a), Santerre (1991) has already summarized the effects of relative tropospheric delay error, as follows (the range is for elevation mask angles of 20° and 10°, respectively):

- For equatorial and mid-latitude sites, the magnification factor ranges from 2.6 to 4.2. In addition, for mid-latitude sites, horizontal translations along the x-axis (north component) also exist but they are insignificant;
- For polar sites, the magnification factor ranges from 3.9 to 6.5.

For the proposed method, i.e., for the geometrical case where only station coordinates are estimated (eqn. 8b), the effects of relative tropospheric delay error are as follows:

- For equatorial sites, the magnification factor ranges from -2.1 to -2.5;
- For mid-latitude sites, the magnification factor ranges from -1.9 to -2.2. In addition, horizontal translations along the x-axis (north component) ranges from 0.6 to 1.2;
- For polar sites, the magnification factor ranges from -3.5 to -4.6.

It is interesting to note, as already pointed out by Beutler et al. (1988) and Geiger (1988), that the translation in the vertical direction (Tz) has opposite signs if the standard data processing or the geometric case is used. The amplification factor for the tropospheric error is about 2 to 4 times larger than the amplification factor associated to intercable bias.

It is possible of course to solve for a tropospheric zenith delay parameter (equations 8c or 8d). This parameter will absorb an unmodelled tropospheric delay (the translations reported in Tables 4 vanish), but it has the consequence to amplify the propagation of measurement noise (random error) into the height component. If the tropospheric refraction error (the major cause of error on small network) can be eliminated without unduly amplifying the confidence ellipsoids associated with station coordinates determination, the proposed technique would be most promising. This question will be addressed in the next sub-section.

3.5 Behaviour of the confidence ellipsoids

To analyse the "geometric" impact of GPS satellite sky distribution on the confidence ellipsoids, the covariance matrices have been scaled to represent the same number of observations for each site and all elevation mask angles. Moreover, the size of the semi-axes of all ellipsoids have been divided by a common number (c_{min}) to bring the value of their semi-minor axes close to unity. In other words, Table 5 and Figures 3 display the relative size (unitless) of the confidence ellipsoids assuming that the number of observations and the observation noise are equal for each simulation run. To get an idea of the accuracy potentially obtainable from standard data processing the reader is referred to section 1.

In Figures 3a, the confidence ellipsoids are plotted for the equatorial, mid-latitude and polar sites, for a 20° elevation mask angle (ζ^{max}: 70°). Figure 3b is similar to Figure 3a but it is valid for a 10° elevation mask angle (ζ^{max}: 80°). The first column of Figures 3a and 3b shows the confidence ellipsoid where station coordinates and clock parameter are estimated; the second column illustrates the confidence ellipsoid where station coordinates only are estimated; and the third column shows the confidence ellipsoid where station coordinates and tropospheric zenith delay parameter are estimated. The confidence ellipsoids, where station coordinates, clock and tropospheric zenith delay parameters are estimated, are not included because of their much larger size. However the size of the semi-axes of their confidence ellipsoids are given in Table 5.

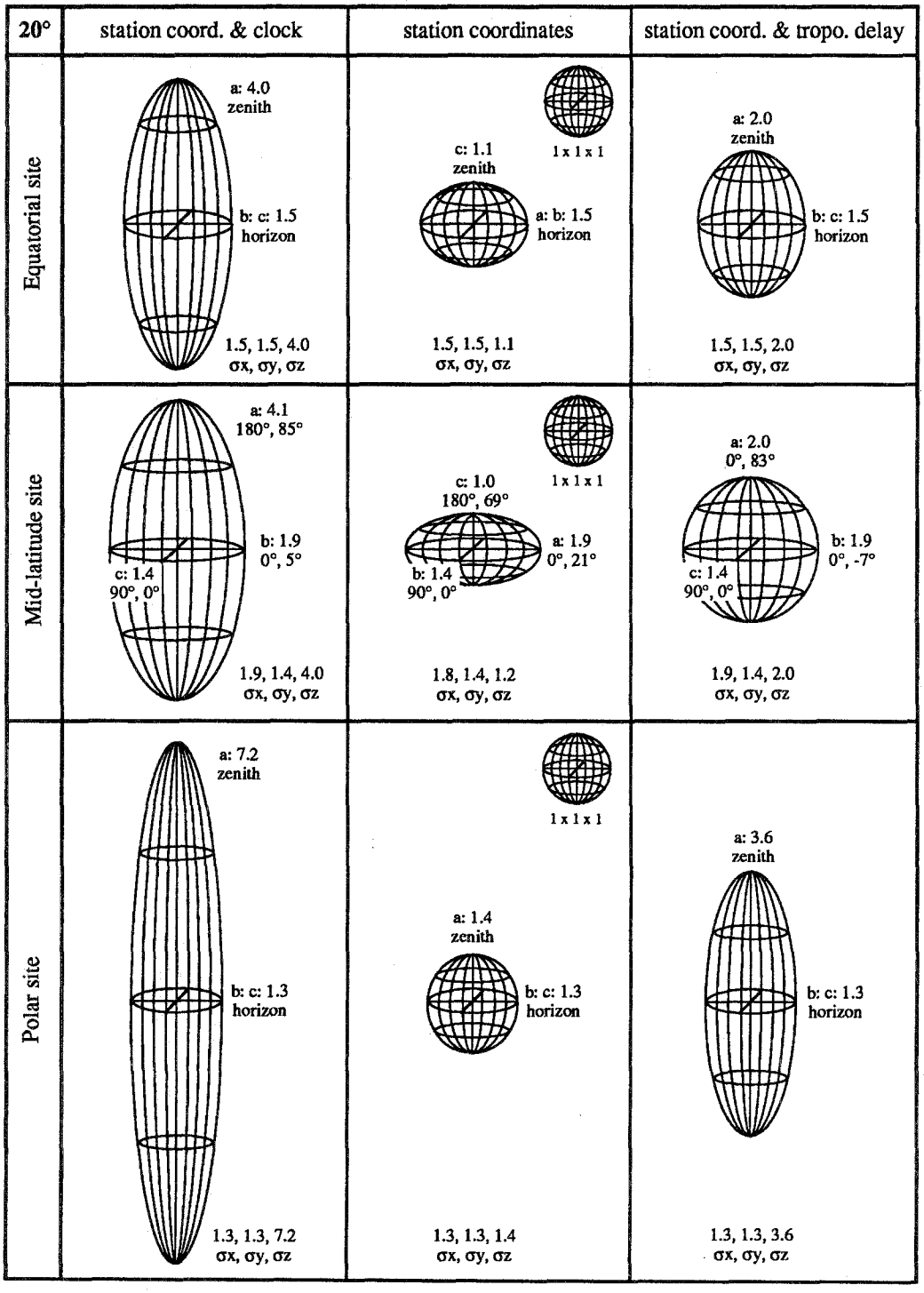

Figure 3a. Confidence ellipsoids for different parameter combinations and an elevation mask angle of 20°.

The number associated with each semi-axis is the "relative" size of the semi-axes of the confidence ellipsoids. The two numbers below the size of the semi-axes (for mid-latitude site) are the azimuth and the elevation of those semi-axes, respectively. The associated standard deviations (σx, σy, σz), which are the values of the intersection of the confidence ellipsoid with the local geodetic coordinate system "north-east-up", are also indicated under each ellipsoid. The unitary spheres allow to better appreciate the relative size of the confidence ellipsoids.

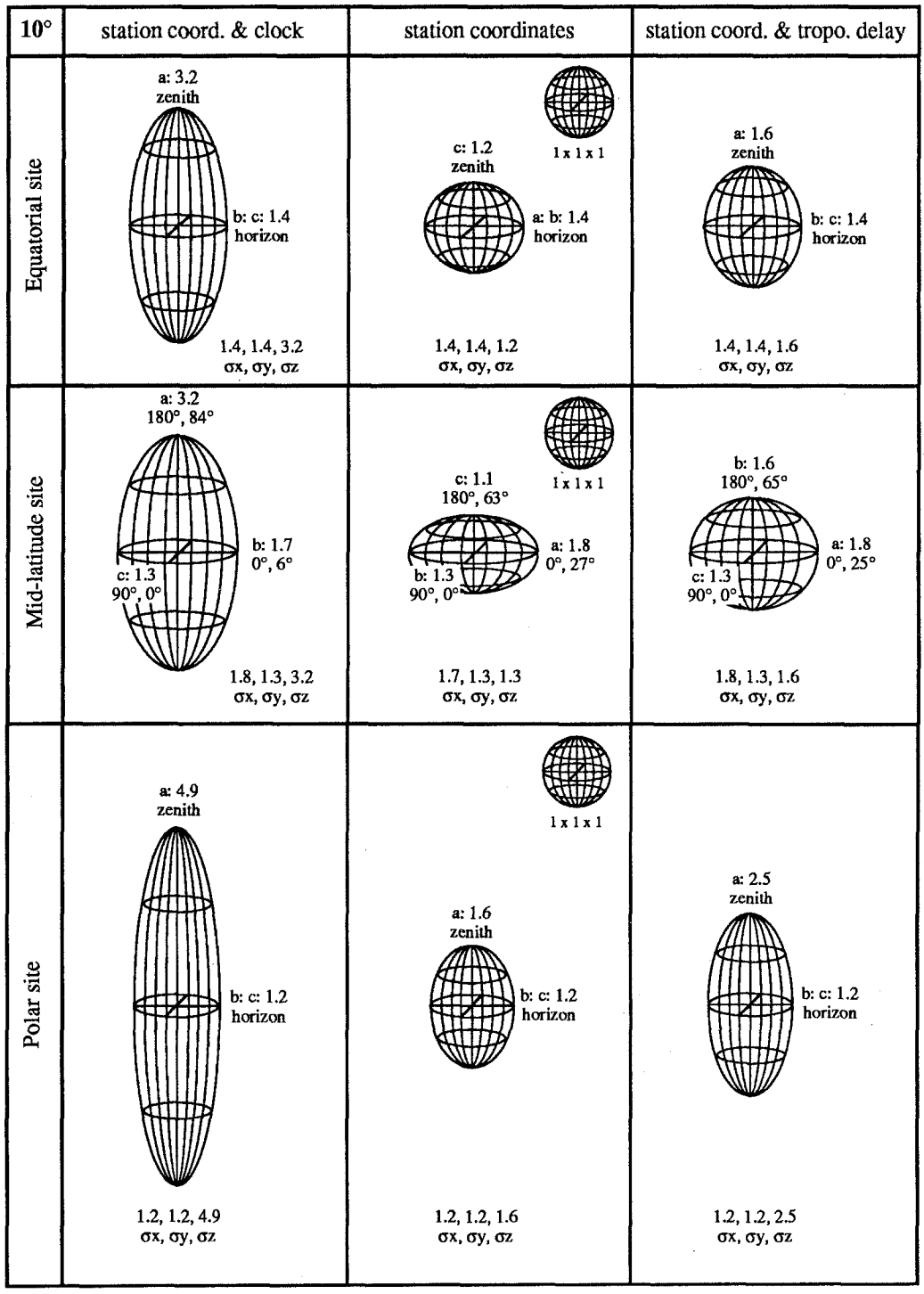

Figure 3b. Confidence ellipsoids for different parameter combinations and an elevation mask angle of 10°.

For standard data processing (eqn. 8a), the general trends are summarized as follows (Santerre 1991):

- For equatorial sites, the height standard deviation is about 2.3 times larger than the horizontal standard deviations for a 10° elevation mask angle (2.7 times larger for 20°);
- For mid-latitude sites, the height standard deviation is about 2.6 times larger than the east standard deviation for a 10° elevation mask angle (3.0 times larger for 20°), moreover the north standard deviation is 1.4 times larger than the east standard deviation. The semi-minor axis points towards the east direction. The semi-major axis does not point towards the zenith, it rather points towards the area containing satellite observations;
- For polar sites, the height standard deviation is about 4.1 times larger than the horizontal standard deviations for a 10° elevation mask angle (5.7 times larger for 20°).

If in addition a tropospheric zenith delay parameter is estimated with the standard processing scheme the ellipsoids are even more elongated towards (or close to) the zenith. These confidence ellipsoids have not been drawn in Figures 3 because of their size. The size of the semi-axes of those confidence ellipsoids is reported in Table 5.

Table 5. Size of the semi-axes of the confidence ellipsoid for standard method with a tropospheric delay parameter.

ζ^{max} :	70°			80°		
	c (σy)	b (σx)	a (σz)	c (σy)	b (σx)	a (σz)
Equatorial	1.5	1.5	14.9	1.4	1.4	7.6
Mid-latitude	1.4	1.9	14.9	1.3	1.8	7.7
Polar	1.3	1.3	39.3	1.2	1.2	14.5

The standard deviations of the horizontal coordinates are not affected, but the size of the semi-major axis has been considerably amplified with respect to the standard method without a tropospheric delay parameter.

- For equatorial and mid-latitude sites, the semi-major axis is magnified by a factor of 2.4 for an elevation mask angle of 10° (a factor of about 3.7 for 20°);
- For polar sites, the magnification factor is 3.0 for an elevation mask angle of 10° (a factor of 5.5 for 20°).

This expansion of the confidence ellipsoid towards the zenith direction is a consequence of the high correlation existing between the relative receiver clock and the relative tropospheric zenith delay parameters and the baseline height component (Santerre 1991).

How will the confidence ellipsoid behave for the proposed method (eqn. 8b)? This can be seen from Figures 3a and 3b (columns 2). The advantage of the proposed method is shown in term of improved height standard deviation with respect to the standard data processing scheme:

- For equatorial sites, the height standard deviation is 2.7 times smaller for a 10° elevation mask angle (3.6 times smaller for 20°);
- For mid-latitude sites, the height standard deviation improved by a factor of 2.5 for a 10° elevation mask angle (3.3 for 20°). The elevation angle of the semi-minor axis is 63° for a 10° mask angle (69° for 20°) close to the middle of the area covered by GPS observations;
- For polar sites, the height standard deviation is 3.1 times smaller for a 10° elevation mask angle (5.1 times smaller for 20°).

The main advantage of the proposed field operation and the associated data processing is the tremendous improvement of height standard deviations. These values are even better than those of the horizontal coordinates, except for polar sites where no observations are available near the zenith. This illustrates that the observations close to the zenith contain significant geometrical information about the height. This may be surprising that the height component becomes as precise as the horizontal coordinates, but let us recall that this sub-section only deals with the propagation of measurement noise (in a covariance analysis, systematic errors are not addressed).

If a relative tropospheric zenith delay parameter is introduced in the least squares adjustment (eqn. 8d), the main effect concerns the height standard deviations. As expected there are elongations of the confidence ellipsoids towards (or close to) the zenith as compared to the proposed method without solving for tropospheric delay parameter (eqn. 8b). Compare columns 2 and 3 of Figures 3a and 3b. Even though, and agreeably, the size of the height standard deviation is of the same order of magnitude as those for the horizontal coordinates (except for polar sites).

Compared to the standard data processing (without tropospheric delay parameter, eqn. 8a), the height standard deviation is still 2 times better for all (equatorial, mid-latitude and polar) sites for elevation mask angles of 10° and 20°. It is remarkable that the orientation of the semi-axes varies significantly, for mid-latitude sites, as a function of elevation mask angle.

Compared to the standard data processing with a tropospheric parameter (eqn. 8c), the improvement is substantial.

- For equatorial and mid-latitude sites, the height standard deviation is 4.8 times smaller for an elevation mask angle of 10° (7.5 times smaller for 20°);
- For polar sites, the height standard deviation is 5.8 times smaller for an elevation mask angles of 10° (10.9 times smaller for 20°).

This means that tropospheric refraction error can be eliminated without unduly amplifying the confidence ellipsoids associated to station coordinates determination, with the proposed method.

4. SUMMARY AND CONCLUSIONS

The proposed field operation consists of collecting data from two (or more) antennae connected to the same receiver. The goal is to eliminate relative receiver clock parameter prior to the least squares adjustments. Clock parameters (implicitly or explicitly estimated with the standard method) are highly correlated with baseline height component and tropospheric parameters. To determine height component to the mm-level, intercable biases must be calibrated at the same level.

The tropospheric delay error is the main error source affecting baseline height components for small network. For the standard method, the tropospheric zenith delay error is mainly magnified in the height component by a factor ranging between 2.6 and 6.5 (for elevation mask angles of 20° and 10°). For the proposed method, the magnification factor ranges between -1.9 to -4.6.

If relative tropospheric zenith delay are suspected to remain after data modelling, a relative tropospheric zenith delay parameter must be estimated. This parameter will absorb the tropospheric error, but this has the consequence to amplify the propagation of measurement noise (random error) into the height component. However, the impact of the addition of a tropospheric parameter is not dramatic for the proposed method.

For standard data processing (without a tropospheric delay parameter), the height standard deviation is 2.3 to 2.7 times larger than the standard deviation of the horizontal coordinates, for equatorial sites and 2.6 to 3.0 times larger for mid-latitude sites. The ratio is 4.1 to 5.7, for polar sites. Moreover, for mid-latitude sites the standard deviation of the north component is 1.4 times larger than the standard deviation of the east component.

The height standard deviation varies quite significantly for different parameter combinations. If a tropospheric parameter is estimated with the standard data processing the height standard deviation becomes 2.4 to 3.7 times larger, for equatorial and mid-latitude sites and 3.0 to 5.5 times larger for polar sites. For the proposed method (without a tropospheric delay parameter) the height standard deviation is smaller (with respect to standard method without a tropospheric delay parameter) by a factor 2.7 to 3.6 for equatorial sites, 2.5 to 3.3 for mid-latitude sites and 3.1 to 5.1 for polar sites. Finally, even if a tropospheric parameter is estimated together with the proposed method, the height standard deviation is still 2 times smaller than the one associated to standard data processing (without a tropospheric delay parameter), for all sites and elevation mask angles. In other words, for the proposed method, the height standard deviations are comparable to those of the horizontal components, even if a tropospheric parameter is solved for (exception of polar sites).

It has been shown that the proposed field operation and its associated data processing significantly improve GPS height determinations compared to standard GPS data processing schemes. The proposed field procedure is more cumbersome (long physical link between antennae and receiver) and requires careful relative cable calibration. However, for special precise applications (e.g., small networks with permanently installed cables) additional efforts can be justified. The benefit is the substantial improvement of GPS height determination. It is hoped that this work will stimulate further, hardware oriented, research along the same lines.

Acknowledgements. This research was funded by the Natural Sciences and Engineering Research Council of Canada Operating Grant: "Amélioration de la détermination des altitudes géodésiques obtenues du système de positionnement GPS". This financial contribution is greatly appreciated. We want to thank graduate student Serge Gosselin for the production of one part of the simulations used in this paper. Finally, we also want to acknowledge Dr. Richard B. Langley from the University of New Brunswick for his help to collect papers and information about fiber optic technology.

References

Beutler G (1992) The 1992 activities of the International GPS Geodynamics Service (IGS). Geodesy and Physics of the Earth, IAG Symposium No. 112, Potsdam, Germany, 5-10 October, in press

Beutler G, Bauersima I, Gurtner W, Rothacher M, Schildknecht T, Geiger A (1988) Atmospheric refraction and other important biases in GPS carrier phase observations. Atmospheric Effects on Geodetic Space Measurements, School of Surveying Monograph No. 12, University of New South Wales, Kensington, Australia, pp 15-43

DeLoach SR (1989) Continuous deformation monitoring with GPS. Journal of Surveying Engineering 115(1): 93-110

Frei E, Beutler G (1990) Rapid static positioning based on the fast ambiguity resolution approach FARA: Theory and first results. Manuscripta Geodaetica 15: 325-356

Geiger A (1990) Influence of phase centre variations on the combination of different antenna types. Proceedings of the Second International Symposium on Precise Positioning with the Global Positioning System, Ottawa, Canada, 3-7 September, pp 466-476

Geiger A (1988) Simulating disturbances in GPS by continuous satellite distribution. Journal of Surveying Engineering 114(4): 182-194

Georgiadou Y (1990) Ionospheric delay modelling for GPS relative positioning. Proceedings of the Second International Symposium on Precise Positioning with the Global Positioning System, Ottawa, Canada, 3-7 September, pp 403-410

Georgiadou Y, Kleusberg A (1988) On carrier signal multipath effects in relative GPS positioning. Manuscripta Geodaetica 13: 172-179

Gurtner W, Beutler G, Botton S, Rothacher M, Geiger A, Kahle H-G, Schneider D, Wiget A (1989) The use of Global Positioning System in mountainous areas. Manuscripta Geodaetica 14: 53-60

Jurgens RD, Rodgers CE (1991) Advances in GPS attitude determining technology as developed for the strategic defense command. Proceedings of the Institute of Navigation GPS-91, Albuquerque, New Mexico, U.S.A., 11-13 September, pp 991-999

Logan RT, Lutes GF, Maleki L (1990) Microwave analog fiber-optic link for use in the Deep Space Network. Jet Propulsion Laboratory, Telecommunications and Data Acquisition Progress Report 42-100, pp 21-33

Primas L, Logan RT, Lutes GF, Maleki L (1990) Distribution of ultra-stable reference frequency signals over fiber optic cable. IEEE Microwave Theory and Technics MTT-S Digest, pp 241-244

Qin X, Gourevitch S, Ferguson K, Kuhl M, Ladd J (1992) Dynamic short baseline calibration and attitude determination using Ashtech 3DF system. Proceedings of the Sixth International Geodetic Symposium on Satellite Positioning, Columbus, U.S.A., 17-20 March, pp 190-199

Remondi BW, Hofmann-Wellenhof B (1989) GPS broadcast orbits versus precise orbits: A comparison study. Global Positioning System: An overview, IAG Symposium No. 102, Edinburgh, Scotland, 7-8 August, pp 203-217

Rocken C, Meertens C (1991) Monitoring selective availability dither frequencies and their effect on GPS data. Bulletin Géodésique 65(3): 162-169

Rothacher M, Beutler G, Gurtner W, Schildknecht T, Wild U (1991) Documentation for Bernese GPS software version 3.3. Astronomical Institute, University of Berne, Switzerland, May

Santerre R (1991) Impact of GPS satellite sky distribution. Manuscripta Geodaetica 16(1): 28-53

Santerre R, Lavoie M (1991) Propagation of GPS errors for ambiguities-fixed and ambiguities-free solutions. Paper presented at the International Union of Geodesy and Geophysics XX General Assembly, Vienna, Austria, 12-23 August, 20 p

Santerre R, Beutler G, Geiger A (1990) GPS error analysis and modelling. Proceedings of the Second International Symposium on Precise Positioning with the Global Positioning System, Ottawa, Canada, 3-7 September, pp 356-372

Santerre R (1989) GPS satellite sky distribution: Impact on the propagation of some important errors in precise relative positioning. Ph.D. dissertation, Department of Surveying Engineering Technical Report No. 145, University of New Brunswick, Fredericton, Canada, 220 p

Santerre R (1988) DIPOP 2.0: Structure, modifications and user guide. Department of Surveying Engineering Technical Memorandum No. 20, University of New Brunswick, Fredericton, Canada

Schreiner WS (1990) A covariance study for orbit accuracy improvement of the GPS satellites using fiber optics tracking. Proceedings of the (U.S.) Institute of Navigation ION GPS-90, Colorado Springs, U.S.A., 19-21 September, pp 563-568

Sjöberg LE (1992) Systematic tropospheric error in geodetic positioning with the global positioning system. Manuscripta Geodaetica 17: 201-209

Thomas JB (1988) Functional description of signal processing in the Rogue GPS receiver. Jet Propulsion Laboratory Publication 88-15, June

Tolman BW, Clynch JR, Coco DS, Leach MP (1990) The effect of selective availability on differential GPS positioning. Proceedings of the (U.S.) Institute of Navigation ION GPS-90, Colorado Springs, U.S.A., 19-21 September, pp 579-586

Tranquilla JM, Colpitts BG (1989) GPS antenna design characteristics for high-precision applications. Journal of Surveying Engineering 115(1): 2-14

Wild U, Beutler G, Gurtner W, Rothacher M (1989) Estimating the ionosphere using one or more dual frequency GPS receivers. Proceedings of the Fifth International Geodetic Symposium on Satellite Positioning, Las Cruces, U.S.A., 13-17 March, pp 724-736

Young AC (1991) The use of optical fibres in radioastronomy. Radio Interferometry: Theory, Techniques and Applications, IAU Coll. 131, Astronomical Society Pacific Conference Series, Vol. 19, TJ Cornwell and RA Perley (eds.), pp 33-41